INTERNATIONAL JOURNAL OF
ADVANCED SCIENTIFIC RESEARCH AND INNOVATION
VOLUME 4, ISSUE 2, 2021, 53 – 73.

Archaeological Bone Properties after treatment with Paraloid / Hydroxyapatite nan composite

Mostafa Samir Abo El-Hassan [a*] ,

Mohamed Marouf [b], **Wael Sabry Mohamed** [c]

a. Conservator, Ministry of Tourism and Antiquities, Egypt.
b. Conservation Department, Faculty of Archaeology,
Sohag University, Egypt.
c. Polymers @ Pigments Department, National Research Centre,
Dokki, Giza, Egypt.

ABSTRACT

There are some archaeological bones resulting from some archaeological excavations, and they have many different manifestations of damage such as brittleness, fragility and weakness, and through the aging of some samples that have been strengthened with In this study, nano-hydroxyapatite concentrations of 1% and 2% + nano-paraloid concentration of 3% dissolved in acetone as an archaeological bone-strengthening substance . Visual assessment and several analytical techniques were used for the evaluation of the selected strengthening material . The analytical techniques are transmission electron microscope (TEM), color change and Pressure strength. The results obtained from transmission electron microscope showed that grain size of nano-hydroxyapatite with nano paraloid was ranging from 51 to 73 nm .

INTERNATIONAL JOURNAL OF
ADVANCED SCIENTIFIC RESEARCH AND INNOVATION
VOLUME 4, ISSUE 2, 2021, 53 – 73.

Visual assessment proved that nano-hydroxyapatite 2% with nano paraloid had some simple changes in appearance. Color change revealed that nano-hydroxyapatite 2% with nano paraloid gave the level of total color differences (ΔE) after thermal and chemical aging with 6.92 and 5.40 respectively compared to the standard sample HA2 gave 2.96. The Pressure strength revealed that nano-hydroxyapatite 2% with nano paraloid after thermal and chemical aging gave Pressure strength 692.91 N/mm2 and 982.15 N/mm2 respectively compared to the standard sample ST gave 694.98 N/mm2. According to these results, we recommend the use of nano-hydroxyapatite 2% with nano paraloid in joining of archaeological Bone.

Key words

Nano-Hydroxyapatite, Archaeological Bones, FTIR, CIE Lab, Thermal Aging

1. INTRODUCTION

bone composition consists of organic material, collagen, non-collagenous protein, lipids and carbohydrates in addition to inorganic mineral as calcium hydroxyapatite Ca10(PO4)6(OH)2. Although its composition varies considerably with age and type of bone. Moreover، when bones are removed from the body they become unstable because they are moved from a relatively closed environment to an open one and can be broken down over time through physical breaking, decalcification and dissolution due to acidic soil and water [1 2-3-4]

The deterioration of the archaeological bone may occur as a result of weathering, fracturing، cracking, surface marks, microbial attack، abrasion, polishing and breakage and these factors occur in isolation or in combination [5, 6]. So the preservation of bone depends not on the length of time has been underground, but the type of bone and burial environment [7]

The development of modern materials and methods for consolidating the artifacts is considered the subject of global interest in research conservation. Moreover, these consolidation materials should be characterization by improved efficiency and potential reversibility [8] . Therefore, the improvement of novel materials or methodologies to consolidate and protect the decayed bone from physical and chemical deterioration is considered very important [9] . Consolidated materials are using to improve the cohesion of archaeological objects. These materials are using when dangerous deterioration patterns and cohesion loss are present.

Paraloid is considered one of the acrylic resins most frequently used in the consolidation of artifacts due to its characteristic mechanical properties and ease of use. Therefore, using a polymer requires dis-solving it in a solvent, such as acetone or toluene [10] . Paraloid B72 is the most used acrylic polymer, although there are numerous kinds of Paraloid formulations available, such as Paraloid B-66 and Paraloid B-67 [11] . When using Paraloid B72 in consolidation, it doesn't cause discoloration for the surface, and thus it is considered acceptable material for cultural heritage preservation. Moreover, Paraloid B72 also increases the water-re- sistance of artifact surfaces [12] .

Hydroxyapatite (HA) has been extensively studied in archaeological strengthening processes , Hydroxyapatite (HA) which has a Ca/P ratio of 1.667 with a chemical formula of Ca10(PO4)6OH2 has achieved the most significant attention because of its compositional similarities to the natural human bone [13], To avoid the disadvantages of using resins, a modern method for the consolidation by nanomaterials has appeared. This new method was mainly used to support mechanical properties [14] . In the recent period, the use of nanomaterials in the field of cultural heritage preservation has become increasingly widespread due to the improvement of the performance of the materials used in treatment.

HA nanoparticles are the materials used to form a protective consoloidation on the surface of artifacts [15] . Modified HA nanoparticles can be hydrophobic, so this material is essential to protect the archaeological objects [16] . The use of HA nanoparticles in the consolidation has a great influence on the physical and mechanical properties. The advantages of this material are related to good chemical stability and resistance to thermal stress [17] .

And through the various examinations and analyzes that you can find, you will find it in watching the size of the bone, knowing the educational methods and means in the total in the world, and preserving, as these examinations include microscopic examination, mechanical and chemical tests, color change test , Measuring the mechanical properties and knowing the bearing capacity of the pressure forces of the samples before the strengthening operations.

FTIR spectroscopy constitutes an excellent tool to characterize the bone matrix because its main components (carbonated hydroxyapatite and collagen) absorb infrared radiation at distinct, almost complementary regions within the 400-4000 cm-1 range [18], In fact, the spectrum of bone exhibits all the most intense bands observed in the spectrum of hydroxyapatite (at 500-700 cm-1 and 900-1200 cm-1) and that of collagen (in the 1200 - 1700 cm-1 and 2800-3700 cm-1 regions), being nearly coincident with the sum of the respective profiles. Nevertheless, there are some new bands (namely at around 870 cm-1 and 1400-1450 cm-1) originated from carbonate substitutions in the crystal lattice of hydroxyapatite [19].

The research reported in this paper was aimed at the preparation and characterization of new formulations of an acrylic consolidant based on Paraloid B72 and containing HA nanoparticles. The present research was carried on seven bone samples treated with two consolidating consentration applied by brushing . This study aims to Knowing the efficiency of the nano-material used in strengthening the bone . Moreover,To identify the effectiveness of the strengthening material through examinations and analyzes. The overall aim is to the establishment of the best strategy for the conservation of this type of cultural objects in museums and archaeological sites.

2. Materials

2.1. Preparation of Bone samples

Archaeological bones samples of sheepwere collected from El-Hawawish excavations in akhmim, sohag, situated at a distance of 12 km from east and north east the city of sohag. This site dates back to the late period, that is about 2000 B.C. After the process of applying Nano Hydroxyapatite with Nano -paraloid, thermal aging was carried out at a temperature of 120 ° C for 10 hours, according to several previous studies carried out by: (Wang, et al, 2010[20],. Hiller, 2003[21],. Kalsbeek and Richter, 2006[22],. Figueiredo, 2010 [23],. Abd el-Maksoud, 2010[24]), and Chemical aging was performed by immersing the samples in a solution of hydrochloric acid (Sigma-Aldrich, Schnelldorf, Germany) At a concentration of 3% in distilled water for a period of one month , according to several previous studies for: (Kalsbeek and Richter, 2006,. Figueiredo, et al, 2012 [25],.Walker, 2011 [26]), In order to evaluate the Nano- paraloid material and compare the samples before and after the aging processes treated for the samples treated of the Nano Hydroxyapatite 1,2% with Nano -paraloid concentration 3% , The samples were divided into 7 samples: a standard sample (ST), a sample treated with 3% nano-paralloid (HA1)(HA2), a treated and thermally aging sample (HA1H)(HA2H), and a chemically aging treated sample (HA1K)(HA2K).

2.2. Preparation of Nano Parloid B 72/HA nanocomposits.

Paraloid B72 was prepared as a co-polymer of methyl methacrylate/ethyl acrylate (MMA/EA) monomers (Aldrich, Darmstadt, Germany) with a composition ratio of 70/30. It was prepared by solution polymerization technique with solid content 3% as a pure copolymer . The polymerization was carried out according to the following procedure: in a 250-mL three-nicked flask, the desired amount of the monomers with the selected composition ratio (70/30 MMA/EA), was stirred with Acetone for 30 min at room temperature using a mechanical stirrer (500 rpm). In addition, the presence of 0.01 g, 0.02 g of HA nanoparticles (nanopowder، < 100 nm particle size (BET), 99.5% trace metals basis obtained from Sigma-Aldrich, Schnelldorf, Germany). Then, the mixture was heated to 80 ºC.

Then، the initiator potassium persulphate (PPS) (0.27 g) (Sigma-Aldrich, Schnelldorf, Germany) dissolved in 50mL of Acetone and Sodium dodecyl sulphate (SDS) as emulsifier dissolved in 45 mL of Acetone was added to the reaction mixture under continuous stirring for 3 h to obtain the solutions of Paraloid B72/ HA nanocomposites. The concentration was selected based on Bone nature and porosity [27] .

3. Methods

3.1.1. ***Transmission electron microscope (TEM) .***

The TEM images were obtained by a JEM-1230 electron microscope operated at 60 KV (JEOL Ltd., Tokyo, Japan). Prior to examination, the sample was diluted at least 10 times by water. A drop of well-dispersed diluted sample was then placed onto a copper grid (200-mesh and covered with a carbon membrane) and dried at ambient temperature. This procedure was conducted at the National Research Centre in Dokki –Egypt.

3.1.2. Fourier-Transform infrared Spectroscopy (FTIR)

Fourier-Transform infrared Spectroscopy (FTIR) was done with an infrared spectrophotometer, the device model is (FTIR.B RUKER, Alpha, made in German), in the range of 4000 - 400 cm-1, in transmission mode. The analysis was performed at the Chemistry Laboratory, Faculty of Science, Sohag University , and the analysis was done after grinding about less than a gram of the sample and adding 0.1 grams (KBR).) and mix them and then compress them together into a hard disk.

3.1.3. Digital Microscope (DM).

Samples were examined with a microscope (Digital Microscope Rohs1600X 2 MP Zoom Microscope 8Led), A digital microscope with a magnification of 100 X was used for samples before and after the hardening operations

3.1.4. Measurement of Mechanical Properties .

Samples were prepared with dimensions of (3 x 2 x 2 cm), The mechanical properties (compression) test was carried out with a Galdabini-Quasar 600-made in Italy and measured in N/mm2 The working conditions (Load Range: 10000N, Extension Range: 10mm, Speed: 50 mm / min, Endpoint: 5.0 mm, preload: 1.0N). The test was conducted at the Antiquities Restoration Center at the Grand Egyptian Museum, Al-haram, Giza، Egypt.

3.1.5. Measurement of Color Change CIE Lab

An Optimatch 3100 ® from the SDL Company was used to measure color change. This procedure was carried out at the National Institute of Standards, Al-haram, Giza، Egypt.

3.1.6. Fourier Transform Infrared Spectroscopy analysis (FTIR).

Bone samples were analyzed using an infrared spectrophotometer Nicolet 380 FT-IR .

4. Results and Discusstion

4.1. Transmission electron microscope (TEM)

From the images, it is clear thatthe particle size of nano Paraloid B-72 ranged between 51 and 73 nm. The image also shows that the prepared nano paraloid has spherical shape nano particles with uniform morphology (Fig. 1). Where nanostructures represent a stage of matter between agglomerated molecules and structures and are typically characterized by a large surface area that affects their physicochemical properties [28].

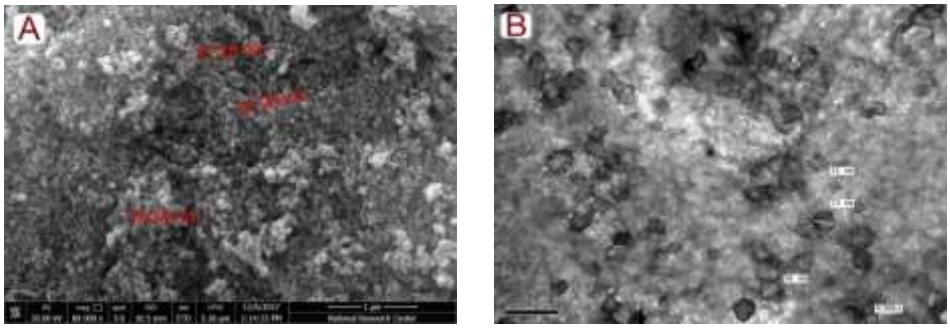

Fig (1) Shows the TEM images of nano Paraloid B-72/HA Nanocomposition. (A) paraloid in nano/HA Nanocomposition form at 1 nm, (B) paraloid in nano/HA Nanocomposition form at 0.2 nm.

INTERNATIONAL JOURNAL OF
ADVANCED SCIENTIFIC RESEARCH AND INNOVATION
VOLUME 4, ISSUE 2, 2021, 53 – 73.

4.2. Fourier-Transform infrared Spectroscopy (FTIR).

FTIR is a common tool in characterizing the surface chemical composition. In this study, it is clear that, the characteristic peaks of Nano Paraloid B-72 as C H stretching (2,900–3,000 cm−1), ester carbonyl stretching (C O) at 1,720 cm−1, C H bending at 1,445 and 1,383 cm−1, while (O H) stretching peak appears in the range of 3,400–3,520 cm−1 and stretching of C O C ester bonds from 1,200 to 1,132 cm−1 have been appeared [29, 30]. As for nano-hydroxyapatite, the appearance of a weak absorption peak for ions Hydroxyl O-H is in the region of (3570.08cm-1) and this motion is Ions in the form of a Stretching vibration, and this is what It was confirmed by previous studies that confirmed the appearance of the (O-H) bundle) within these limits. The absorption band that lies in the region (3402.64cm-1) denotes Water absorption by hydroxyapatite, either group Phosphates (PO4) are shown in FTIR spectroscopy, moving in two motions، The first movement is in the form of asymmetric stretching for O-P-O, and the peaks of this type from 1555 - 1505 cm-1 and the other movement is in the form of asymmetric stretching of curvature Asymmetric bending Peak absorbance is shown This group is at (563 1-cm) and previous research has confirmed that this Motion gives absorbance at wavelengths of about (550-570 cm-1) [31, 32]. (Fig. 2).

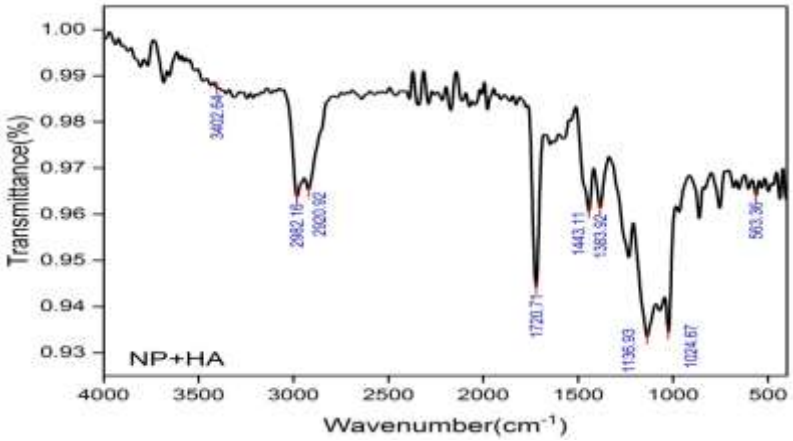

Fig (2) Fourier-Transform infrared Spectroscopy (FTIR) the characteristic peaks of Nano Paraloid B-72/HA nanocomposites

4.3. Digital Microscope (DM).

Fig (3) DM shows samples of for nano-hydroxyapatite concentrations of 1% + nano-paraloid concentration of 3% where (A) represents the standard sample ST and (B) the Strengthening sample HA1 and (C) a thermally aging Strengthening sample HA1H (D) a chemically aging Strengthening sample HA1K

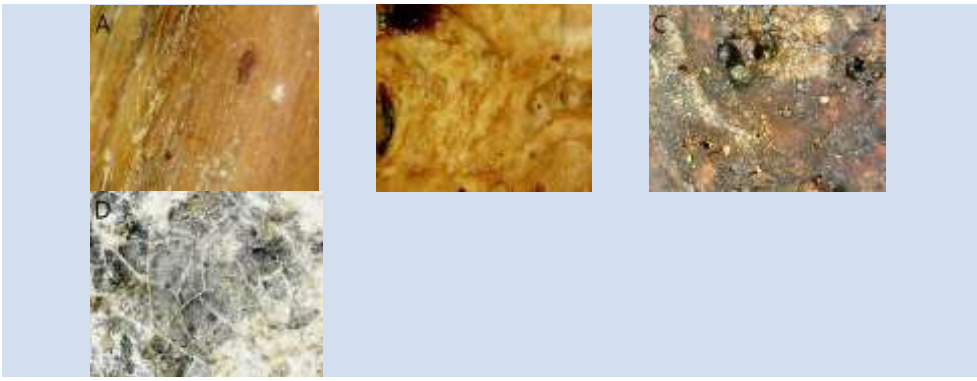

Fig (4) DM shows samples of for nano-hydroxyapatite concentrations of 2% + nano-paraloid concentration of 3% (A) represents the standard sample ST and (B) the Strengthening sample HA2 and (C) a thermally aging Strengthening sample HA2H (D) a chemically aging Strengthening sample HA2K

INTERNATIONAL JOURNAL OF
ADVANCED SCIENTIFIC RESEARCH AND INNOVATION
VOLUME 4, ISSUE 2, 2021, 53 – 73.

4.4. Measurement of Mechanical Properties.

Table (1) shows the results of pressure tests for nano hydroxyapatite concentrations of 1,2 % + nano-paraloid concentration of 3%

M	Sample	Stress endurance (kg/cm2)	Stress endurance (N/mm2)
1	ST	70 .86	694.98
2	HA1	203.77	1998.36
3	HA1H	160.09	1570.86
4	HA1K	180.94	1774.51
5	HA2	95.41	935.65
6	HA2H	70.65	692.91
7	HA2K	100.15	982.15

From the previous table (1) The results of measuring the mechanical properties showed varying changes in the values of the mechanical properties of the samples treated with hardening compared to the standard sample, whether thermally aging samples after hardening or chemically aging samples after hardening. The results came as follows: As the results of measuring the pressure strength of the reinforced samples and comparing them with the standard sample (ST) (70.86 kg/cm2), it was found that some samples had an increase in the ability to resist pressure forces, as the sample of the nano-hydroxyapatite sample recorded a concentration of 1% (HA1) (203.77 kg). / cm2), followed by a sample of nano-hydroxyapatite with a concentration of 2% (HA2) (95.13 kg / cm2), and the results of the pressure strengths of the thermally aging and hardening samples compared to the standard sample (70.86 kg / cm2) (ST),

where it was found that some samples had A slight effect on the mechanical properties after exposure of samples reinforced with nanomaterials to heat aging, where the reinforcing sample of nano-hydroxyapatite recorded the highest concentration of 1% (HA2H) (160.09 kg/cm2), then followed by a sample of nano-hydroxyapatite concentration of 2% (HA2H) (70.65 kg/cm², and the results of the compressive strength of the chemically aging and reinforcing samples compared to the standard sample (70.86 kg/cm² (ST), where it was found that some samples had an increase in mechanical properties and their ability to resist compressive forces compared to the standard sample after exposure to samples Reinforced with nanomaterials for chemical aging, a sample was recorded Nano-hydroxyapatite 1% concentration at the highest pressure resistance (HA1K) (180.94 kg / cm2), then followed by a sample of nano-hydroxyapatite 2% concentration (HA2K) (100.15 kg / cm2).

4.5. Measurement of Color Change CIE Lab

Table (2) shows the chromatic change values of nano-hydroxyapatite concentrations of 1,2 % + nano-paraloid concentration of 3%.

M	S	L	A	B	ΔL	Δa	Δb	ΔE
1	ST	52.30	4.11	8.64	-	-	-	-
2	HA1	46.06	-0.68	2.34	-6.24	-4.80	-6.30	10.08
3	HA1H	44.80	-0.89	2.02	-7.50	-5.00	-6.62	11.18
4	HA1K	60.13	4.33	10.84	7.83	0.22	2.20	8.13
5	HA2	49.52	3.28	8.02	0.65	-0.83	-0.62	2.96
6	HA2H	47.16	1.35	4.90	-5.14	-2.76	-3.74	6.92
7	HA2K	54.95	0.50	4.67	0.65	-3.61	-.3.97	5.40

From the previous table (2) It is clear that the values of (L) in the samples (HA2K) and (HA1K) were (54.95) and (60.13), respectively, as they had a fading as a result of their increase in the (L) values of the standard sample ST, which was (52.30), while the samples (HA1) And (HA1H), (HA2) and (HA2H), which gave the values of (46.06),

(44,80), (49.52) and (47,16), respectively, and it was dark in medium compared to the standard sample. As for the values (Δa), the sample HA1K was (0.22) which gave the sample a color change to the red color slightly and not noticeably, while the samples (HA2) and (HA2H) gave values of (-0.83) and (-2.76) respectively and gave a chromatic change to the color Green is slight and unnoticeable, while samples (HA2K), (HA1) and (HA1H), which gave values of (-3.61), (-4.80) and (-5.00), respectively, and gave a color change to green in a medium and unnoticeable degree, and As for the values (Δb), the sample HA1K was (2.20) which gave a slight and unnoticeable color change for the sample to yellow, while the sample (HA2) was (-0.96) gave the sample a slight and unnoticeable color change to blue. (HA2H) and (HA2K) samples, which gave values (-3.74). and (-3.97) respectively and gave a color change to blue in a medium and unnoticeable degree, while samples (HA1) and (HA1H) gave values of (-6.30) and (-6.62) respectively and gave a significant and noticeable color change to blue.

As for the values of (ΔE), the samples (HA2) gave (2.96), which gave a slight and unnoticeable total color change, while the samples (HA2H), (HA2K) and (HA1K) had their values (6.92), (5.40), and (8.13). It gave a significant and noticeable total chromatic change for the sample, while the samples (HA1) and (HA1H) gave the values of (10.08) and (11.18), respectively, and gave a very clear and large total chromatic change for the samples.

4.6. **Fourier Transform Infrared Spectroscopy analysis (FTIR).**

And through Fig No. (5) shows the components of hydroxyapatite, it appeared in the ranges of 559 and 598 cm-1, which corresponds to the asymmetric bending vibrations of the spectrum of phosphate groups (O-P-O) for 1% hydroxyapatite samples in the standard sample ST, as well as samples HA1, HA1H, HA1K , where there was an increase in the vibration intensity of samples HA1, HA1H, and a decrease in the vibration intensity of samples HA1K compared to the standard sample, moreover, the absorption at 1017 cm-1 corresponds to the asymmetric expansion of the O-P-O group, where there was an increase in the vibration intensity of samples HA1 , HA1H, and a decrease in the intensity of The vibration of the HA1K sample compared to the standard sample, and it should also be noted that acidic phosphate (-HPO4),

which is a frequent anionic substituent in the crystal lattice of hydroxyapatite, was found at a band of 1174 cm−1 in the standard sample and not present in the rest of the samples[33] .

As for the carbonate groups -CO3, the distinct bands appeared at 870-880 cm-1 (as a single band) and at 1400-1450 cm-1 (as a double band), where they appeared at a band of 870 cm-1, which corresponds to the asymmetric curvature, as it increased In the vibration intensity compared to the standard sample, and it appeared at the ranges of 1410 cm-1 where it corresponds to the expansion of the asymmetric CO3 and CH2 group and 1457 cm-1 where it corresponds to the expansion of the CO3 group and the curvature of the asymmetric CH2 group of the standard sample, where an increase in the intensity of vibration occurred For HA1H, HA1K samples, and a decrease in the vibration intensity of HA1 sample compared to the standard sample, this range is characteristic of B-type apatite, so most of the absorption from phosphate vibrations is clearly observed in both bone spectra of hydroxyapatite, and it can be seen that the functional groups of the phosphate and carbonate, the main component of hydroxyapatite, are not affected and there is no loss in any of constituent domains of these functional groups [34-35].

As for the second component of bone which is collagen the organic component of bone, the amide I band located in the range 1600-1700 cm-1, is the strongest adsorption band in collagen, mainly caused by C=O stretching vibration (with a slight contribution from CN stretching), Where it is found in the ranges of 1645, 1645, 1647 and 1641 cm-1 for samples ST , HA1, HA1H, HA1K respectively[36].

Amide II, which is present at the range 1500-1600 cm-1 in collagen, is mainly caused by a combination of bending and CN-stretching vibrations of the peptide bonds, and is present in the ranges of 1551, 1541, 1559 and 1541 cm-1 for samples ST, HA1, HA1H, HA1K Respectively, the Amide III band (1200-1300 cm-1), mainly from CN extension and NH curvature, is found in the 1274 cm-1 range for the standard ST sample and in the 1224, 1247 and 1237 bands for all HA1, HA1H, HA1K samples Respectively, where there was an increase in the intensity of vibration for all samples compared to the standard sample ST in all amide bands [37].

The Amide A and Amide B bands are located, close to 3300 cm-1 and 3100 cm-1 respectively, from the extended base band of NH, wherein Amide A is present in the 3284, 3278, 3288 and 3274 cm-1 bands for all samples ST, HA1 ,HA1H, HA1K, respectively, and it can be observed the presence of the functional groups of the main component of collagen (Amide I Amide II, Amide III, Amide A) in all samples compared to the standard sample, and we also notice an extension in the links of the main functional groups, which refers to the chemical structure of methylmeth Acrylates in nano-paralloid (CH), where the bonds extended between 2800-3100 cm-1, also had an increase in the intensity of absorption in all samples [38].

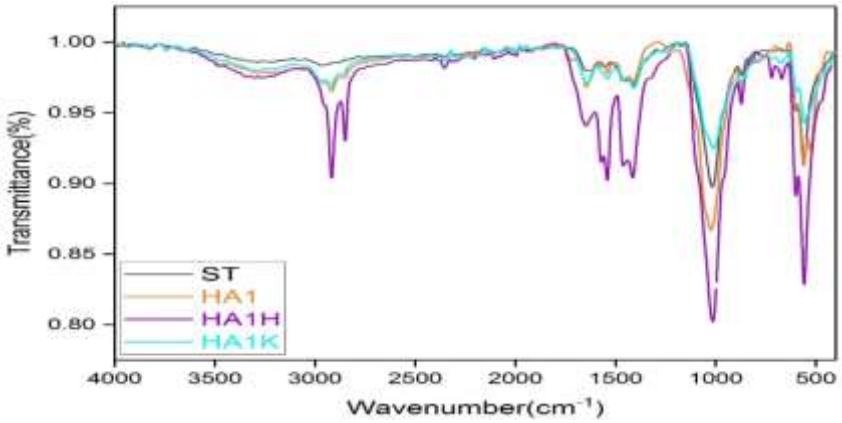

Fig (5) shows FTIR Analysis of nano-hydroxyapatite concentrations of 1% + nano-paraloid concentration of 3% .

And through the Fig No. (5) shows the components of hydroxyapatite, it appeared in the ranges of 559 and 598 cm-1, which corresponds to the asymmetric bending vibrations of the spectrum of phosphate groups (O-P-O) for samples of hydroxyapatite concentration 2% in the standard sample ST, as well as samples HA2, HA2H, HA2 K, where there was an increase in the vibration intensity of all samples compared to the standard sample, moreover, the absorption at 1017 cm-1 corresponds to the asymmetric expansion of the O-P-O group where there was an increase in the vibration intensity of all samples compared to the standard sample, and another band appeared for the O-P-O group at 1057 cm- 1 in the HA2K sample, and an absorption band appeared at 990 cm-1, which is a band that corresponds to a symmetric expansion of the O-P-O phosphate group in the HA2K sample. It was found at a range of 1174 cm-1 in the standard sample and in the rest of the samples at a range of 1139 cm-1.

As for the carbonate groups -CO3, the distinct bands appeared at 870-880 cm-1 (as a single band) and at 1400-1450 cm-1 (as a double band), where they appeared at a band of 870 cm-1, which corresponds to the asymmetric curvature, as it increased In the vibration intensity compared to the standard sample, and it appeared at the ranges of 1410 cm-1 where it corresponds to the expansion of the asymmetric CO3 and CH2 group and 1457 cm-1 where it corresponds to the expansion of the CO3 group and the curvature of the asymmetric CH2 group of the standard sample, where an increase in the intensity of vibration occurred For HA2, HA2H samples, and a decrease in the vibration intensity of HA2K sample compared to the standard sample, this range is characteristic of B-type apatite, so most of the absorption from phosphate vibrations is clearly observed in both bone spectra of hydroxyapatite, and the doubly degraded mode can be observed For hydroxyapatite at less than 500 cm-1, it appeared in the HA2H sample at the 439 cm-1 band, and in the HA2K sample in two bands at 439 and 471 cm-1.

As for the second component of bone, collagen, the organic component of bone, many vibrational domains originated from the amide groups that form the peptide bonds of this protein. Typically characteristic vibrations of amide groups in collagen, the amide I band located in the 1600-1700 cm-1 range, is the strongest adsorption band in collagen, mainly caused by the C=O stretching vibration (with a slight contribution from CN stretching), It is found in the 1645, 1645, 1647 and 1647 cm-1 bands for samples ST, HA2, HA2H, HA2K respectively.

Amide II, which is present at the range 1500-1600 cm-1 in collagen, is mainly caused by a combination of bending and CN-stretching vibrations of the peptide bonds, and is present in the ranges of 1551, 1555, 1559 and 1543 cm-1 for samples ST, HA2,HA2H, HA2K Respectively, the Amide III band (1200-1300 cm-1), mainly from CN extension and NH curvature, is found in the 1274 cm-1 range for the standard ST sample and in the 1234 cm-1 bands for HA2 sample, and it’s not present in the rest of samples, where there was an increase in the intensity of vibration for all samples compared to the standard sample ST in all amide bands.

The Amide A and Amide B bands are located, close to 3300 cm-1 and 3100 cm-1, respectively, from the extended baseband of NH, with Amide A present in the 3284, 3288, and 3286 cm-1 bands for ST, HA2H, HA2K and non-NH samples. Its presence in the HA2 sample, and the deteriorating state of collagen can be observed through the loss of Amide III in samples HA2K, HA2H and loss of Amide A in sample HA2, and we also notice an extension in the bonds of the main functional groups, which refers to the chemical structure of methylmethacrylate in nano paraloid which is (CH) where the bonds extended between 2800-3100 cm-1.

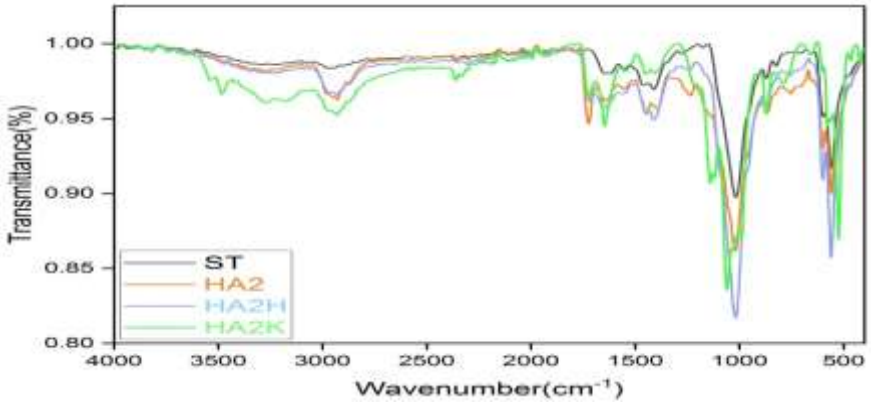

Fig (6) shows FTIR Analysis of nano-hydroxyapatite concentrations of 2% + nano-paraloid concentration of 3% .

C0nclusion

It is known that the archaeological bones are exposed to many damages due to the burial environment extracted from them or due to poor storage in the museum stores and the various effects of the factors of damage. And the effectiveness of this material in the processes of strengthening the archaeological bones, the compressive strength of samples reinforced with Nano Hydroxtapatite 1%, there was an increase in the compressive strength of the HA1 reinforcement sample and the thermally aged and HA1H reinforcement sample. Chromatic change: The total chromatic change of the samples in ΔE occurred to a very large and noticeable degree. Results of FTIR analysis , the chemical copmposition of samples that had been strengith with Nano Hydroxtapatite 1%, material not change in all the thermally and chemically aging samples , it can be seen that the functional groups of the phosphate and carbonate, the main component of hydroxyapatite, are not affected and there is no loss in any of constituent domains of these functional groups,

and it can be observed the presence of the functional groups of the main component of collagen (Amide I Amide II, Amide III, Amide A) in all samples compared to the standard sample .

References

1. Abdel-Maksoud G.,(2010); Comparison between the Properties of "Accelerated Aged" bones and archaeological bones. Journal of Mediterranean Archaeology and Archaeometry, 10 (1), pp.89–112.
2. Pestle W.J،.Colvard M.(2012); Bone collagen preservation in the tropics: a case study from ancient Puerto Rico, J. Archaeol. Sci. 39 (7), 2079 -2090 .
3. Barth H.D., Zimmermann E.A., Schaible E., Tang S.Y., Alliston T. and Ritchie R.O.,(2011); Characterization of the effects of X-ray irradiation on the hierarchical structure and mechanical properties of human cortical bone, Biomaterials 32 (34،(8904–8892.
4. Walker G.T., (2008); The chemical and microbial degradation of bones and teeth,ch 1, Adv. Human Paleopathol. Publisher: Wiley, Editors: Ron Pinhasi and Simon Mays 3–30.
5. Wyszecki G. and Stiles W. S.(2000); Color Science Concepts and Methods. Quantitative Data and Formulae. Second Edition, JohnWiley & Sons، Inc. New York.
6. Fuchs R. K., Allen M. R., Ruppel M. E., Diab T., Phipps R. J., Miller L. M. and Burr D. B, (2008) ; In situ examination of the time-course for secondary mineralization of Haversian bone using synchrotron Fourier transform infrared micro spectroscopy. Journal of Matrix Biology, 27 , pp.134-141.
7. Nielsen-Marsh C.M. and Mhedges R. E., (2000) ; Patterns of diagenesis in bone I: the effects of site environments, Journal of Archaeological Science, 27(12),pp. 1139-1150.
8. Traistaru, A. T., Timar, M. C., Campean, C., Coroitoru, C., Sandu, I. (2012) Paraloid B72 Versus Paraloid B72 with Nano-ZnO Additive as Consolidants for Wooden Artefacts. MATERIALE PLASTICE, Vol. 49، No. 4, pp. 393-300.
9. Adam, O., Hemada, S., Abd El-Hady, M. (2015) Durability of decorative stones and other construction materials of Al-Tanbogha Al-Mardany mosque (1340 A.D) 14TH century in Cairo. Egyptian. Journal of Archaeological and Restoration Studies, vol. 5, No. 1, pp. 21-29.

10. Vinçotte, A., Beauvoit, E., Boyard, N., Guilminot, E. (2019) Effect of solvent on Paraloid ® B72 and B44 acrylic resins used as adhesives in conservation. Heritage Science, Vol. 42, No. 7, pp.1-9.
11. Constancio, C., Franco, L., Russo, A., Anjinho, C., Pires, J., Vaz, M. F., Carvalho, A. P. (2010) Studies on Polymeric Conservation Treatments of Ceramic Tiles with Paraloid B-72 and Two Alkoxysilanes. Journal of Applied Polymer Science, Vol. 116, No. 5, pp. 2833–2839.
12. Kaplana, Z., Bökea, H., Sofuoglub, A., İpekoğlua, B. (2019) Long term stability of biodegradable polymers on building limestone. Progress in Organic Coatings, Vol. 131, pp. 378-388.
13. Kerim Emre ÖKSÜZ, (2018); Properties of Nano Hydroxyapatite Powder Derived from Human Teeth, Chemistry Research Journal, 3(6), pp. 76-81.
14. Salama, K. K., Ali, M. F., El-Sheikh, S. M. (2018) The Different Influence of Nano Materials on Pigments. Scientific Culture, Vol. 4, No. 3, pp. 1-7.
15. Aldosari, M. A., Darwish, S. S., Adam, M. A., Elmarzugi, N. A., Ahmed, S. M. (2019) Evaluation of preventive performance of kaolin and calcium hydroxide nanocomposites in strengthening the outdoor carved limestone. Archaeological and Anthropological Sciences, Vol. 11, pp. 3389-3405.
16. Ruffolo, S. A., La Russa, M. F., Malagodi, M., Rossi, C. O., Palermo, A. M., Crisci, G. M. (2010) ZnO and ZnTiO3 nanopowders for antimicrobial stone coating, Applied Physics A, Vol. 100, pp. 829-834.
17. Ditaranto, N, van der Werf, ID, Picca, RA, Sportelli, MC, Giannossa, LC, Bonerba, E., Tantillo, G., Sabbatini, L (2015) . Characterization and behaviour of ZnO-based nanocomposites designed for the control of biodeterioration of patrimonial stoneworks. New Journal of Chemistry, Vol. 39, pp. 6836-6843.
18. Verdelis, K., Lukashova, L., Wright, J. T., Mendelsohn, R., Peterson, M. G. E., Doty, S., et al. (2007). Maturational changes in dentin mineral properties. Bone, 40(5),pp. 1399-1407.
19. M.M. Figueiredo, J.A.F. Gamelas and A.G. Martins,(2012) ; Characterization of Bone and Bone-Based Graft Materials Using FTIR Spectroscopy, Infrared Spectroscopy - Life and Biomedical Sciences, Prof.Theophanides Theophile (Ed.),pp. 315-338. ISBN: 978-953-51-0538-1.

20. X. Y. Wang, Y. Zuo, D. Huang, x. d. Hou, and Li. Y. Boa, (2010); " Compartive Study on Inorganic Composition and Crystallographic Properties of Cortical and Cancellous Bone, Biomedical and Environmental Sciences 23, pp.473-480.
21. J. C. Hiller, T. J. U. Thompson, M. P. Evison, A. T. Chamberlain, T. J. Wess, (2003) ; " Bone mineral change during experimental heating: an X-ray scattering investigation. Biomaterials 24. pp.5091-5097.
22. N. Kalsbeek, and J. Richter,(2006) ; Preservation of burned bones: an investigation of effects of temperature and PH on hardness, Studies in conservation, Vol.51, No.2, pp. 123-138.
23. M. M. Figueiredo, A. Fernando, G. Martins, J. Freitas, F. Judas, and H. Figueiredo, (2010) ; " Effect of the calcination temperature on the composition and microstructure of hydroxyapatite derived from human and animal bone, Ceramics international 36, pp.2383-2393.
24. G. Abdel-Maksoud,(2010); " Comparison between the properties of "Accelerated Aged" bone and archaeological bones, Journal of Mediterranean archaeology and archaeometry, Vol.10 (1), pp. 89-112.
25. M. M. Figueiredo, J. A. F. Gamelas, and A. G. Martins, (2012); " Charachterization of bone abd bone-based graft materials using FTIR Spectroscopy, Infrared spectroscopy – life and biomedical sciences(Portugal), pp.316.338.
26. G. T. Walker, (2011); " The mechanical properties of artificially aged bone: probing the nature of the collagen-mineral bond, palaeogeogrphy, palaeoclimatology ,palaeoecology 310, Pp.17-22.
27. Mohamed Moustafa Ibrahim , Wael Sabry Mohamed, and Hamdy Mohamed Mohamed, (2021) ; EXPERIMENTAL STUDY FOR EVALUATION OF PARALOID® B72 AND ITS NANOCOMPOSITE WITH NANO TiO2 AND NANO ZnO FOR CONSOLIDATION OF POTTERY SAMPLES, SCIENTIFIC CULTURE, Vol. 7, No. 2, pp. 101-111.
28. K. J. Klabunde, R. S. Mulukutla, (2001) ; "Chemical and Catalytic Aspects of Nanocrystals", In:Nanoscale Materials in Chemistry, Edited by K. J. Klabunde, John Wiley and Sons, Inc. Kansas, PP.232-261.

29. J. I. Morán, V. A. Alvarez, V. P. Cyras, & A. Vázquez, (2018); " Extraction of cellulose and preparation of nanocellulose from sisal fibers". Cellulose, 15, PP.149–159 .
30. N. H. El-sayed , et al, (2020); "Preparation and characterization of Paraloid B-72/TiO2 nanocomposite and their effect on the properties of polylactic acid as strawberry coating agents" , Journal of Food Saftey, Wiley Periodicals LLC, pp.1-14. https://doi.org/10.1111/jfs.12838.
31. J. Venkatesan, B. Lowe, P. Manivasagan, K.Kang, E. P. Chalisserry, S. Anil and D. G. Kim, (2015); "Isolation and Characterization of Nano-Hydroxyapatite from Salmon Fish Bone", Materials, Vol. 8,pp. 5426-5439.
32. D. Gopi, J. Indiraa, L., S. Kannand and J.M. Ferreira,(2010); "Spectroscopic characterization of nanohydroxyapatite synthesized by molten salt method", Spectrochimica Acta, 77 , pp.545–547.
33. El-Hussein, A., Marzouk, A., & Harith, M. A. (2015);.Discriminating crude oil grades using laser-induced breakdown spectroscopy. Spectrochimica Acta Part B: Atomic Spectroscopy, 113, pp. 93–99. https://doi.org/10.1016/j.sab.
34. Janik, L. J., Merry, R. H., Forrester, S. T., Lanyon, D. M., & Rawson, A. (2007). Rapid prediction of soil water retention using mid infrared spectroscopy. Soil Science Society of America Journal, 71(2),pp. 507–514. https://doi.org/10.2136/ sssaj2005.0391
35. Tinti, A., Tugnoli, V., Bonora, S., & Francioso, O. (2015). Recent applications of vibrational mid-infrared (IR) spectroscopy for studying soil components: A review. Journal of Central European Agriculture, 16(1), pp. 1–22. https://doi.org/10.5513/ JCEA01/16.1.1535
36. Paschalis, E. P., Verdelis, K., Doty, S. B., Boskey, A. L., Mendelsohn, R., & Yamauchi, M. (2001). Spectroscopic characterization of collagen cross-links in bone. Journal of Bone and Mineral Research, 16(10), pp. 1821–1828.
37. Lumsdon, D. G., & Fraser, A. R. (2005). Infrared spectroscopic evidence supporting heterogeneous site binding models for humic substances. Environmental Science & Technology، 39(17),pp. 6624–6631. https://doi.org/10.1021/es050180i.

38. M.M. Figueiredo, J.A.F. Gamelas and A.G. Martins (2012). Characterization of Bone and Bone-Based Graft Materials Using FTIR Spectroscopy, Infrared Spectroscopy - Life and Biomedical Sciences, Prof. Theophanides Theophile (Ed.),pp.315-338. ISBN: 978-953-51-0538-1.